frontiers | Frontiers in Earth Science

TYPE Original Research
PUBLISHED 28 November 2025
DOI 10.3389/feart.2025.1690793

OPEN ACCESS

EDITED BY
Li Ang,
Jilin University, China

REVIEWED BY
Steven J. Schatzel,
Centers for Disease Control and Prevention (CDC), United States
Yifan Gu,
Southwest Petroleum University, China
Yuguang Hou,
China University of Geosciences Wuhan, China

*CORRESPONDENCE
Dishu Chen,
cds1003chengdu@163.com
Jinxi Wang,
m17347807272@163.com

RECEIVED 22 August 2025
REVISED 24 October 2025
ACCEPTED 31 October 2025
PUBLISHED 28 November 2025

CITATION
Yao Y, Tian X, Liu M, Liao Y, Peng J, Guo D, Zhang Y, Zhang Y, Tuo C, Chen D, Chen C, Wang J and He T (2025) Sedimentary environmental constraints on organic matter enrichment in the coal-bearing Permian Longtan Formation: a case study from NT1H Well, Central Sichuan Basin, China. *Front. Earth Sci.* 13:1690793. doi: 10.3389/feart.2025.1690793

Sedimentary environmental constraints on organic matter enrichment in the coal-bearing Permian Longtan Formation: a case study from NT1H Well, Central Sichuan Basin, China

Yongjun Yao[1,2], Xuesong Tian[1,3,4], Maoyao Liu[1,3], Yisha Liao[2], Junfei Peng[1,3,4], Dongxin Guo[1,4], Ye Zhang[1,3], Yuelei Zhang[1,3,4], Cong Tuo[2], Dishu Chen[1,3,4]*, Chaogang Chen[5], Jinxi Wang[1,3]* and Tingpeng He[1,3]

[1]Key Laboratory of Shale Gas Exploration, Ministry of Natural Resources, Chongqing Institute of Geology and Mineral Resources, Chongqing, China, [2]Chongqing Gas Field, PetroChina Southwest Oil and Gas Field Company, Chongqing, China, [3]National and Local Joint Engineering Research Center of Shale Gas Exploration and Development, Chongqing Institute of Geology and Mineral Resources, Chongqing, China, [4]Chongqing Huadi Resources and Environment Technology Co., Ltd., Chongqing, China, [5]Sichuan Energy Investment Oil and Gas Exploration and Development Co., Ltd., Chengdu, China

The Permian Longtan Formation (burial depth >2000 m) is a major hydrocarbon-producing unit in central Sichuan Basin, China, and an important heterogeneous unconventional gas reservoir. However, the control of sedimentary environment on organic matter enrichment in its coal-bearing strata remains unclear, hindering deep coalbed methane (CBM) exploration in this region. This study analyzed core samples from NT1H Well using petrological and geochemical methods (e.g., thin-section, X-ray diffraction, trace elements, total organic carbon, FE-SEM, and macerals) to characterize the middle-lower Longtan Formation. It examined how sedimentary environments influence organic matter enrichment and generating-gas capacity (abundance, maturity, and component), revealing key controls. Results show the lithologies in the middle-lower Longtan Formation include mudstone/shale, silty mudstone, and tuffaceous-muddy siltstone-standstone interbedded with multiple thin coal seams, mainly containing clay minerals, quartz, pyrite, and siderite. Horizontal bedding, horizontal-wavy bedding, and parallel bedding are common. Coal seams and their surrounding mudstones/shales have higher organic matter abundances than muddy siltstones-sandstones, indicating strong capacities of organic matter accumulation and gas generation. Coal seams, dominated by vitrinite with minor inertinite, show the highest organic abundance and maturity (TOC 43.76 wt% to 77.97 wt%, R_0 >2.5%) than surrounding mudstones/shales. The coal-bearing strata is mainly assigned to lagoon deposits, with two microfacies: sandy-muddy lagoon and peat swamp. The peat swamp is formed by a rapid transformation of muddy lagoon, with sufficient supply of terrestrial materials. These results reveal that the peat swamp microfacies, characterized by weak hydrodynamics and anoxic-to-reducing conditions, is the primary control on the development of multiple

thin coal seams, mudstone/shale, and carbonaceous shale, constraining the degree of organic matter enrichment. This study clarifies the sedimentary environmental constraint on organic matter enrichment in the coal-bearing strata, providing a geological basis for evaluating deep CBM resources in central Sichuan Basin.

KEYWORDS

deep CBM, organic matter enrichment, sedimentary microfacies, coal-bearing Longtan formation, central Sichuan Basin

1 Introduction

Coalbed methane (CBM) is a critical component of unconventional natural gas. As the continuously increasing demand for clean energy, it has garnered growing attention (Cao et al., 2014; Dai and Gong, 2018; Liu et al., 2018; Qin, 2018; 2021; Vinson et al., 2019; Jamieson et al., 2020; Lu et al., 2021; Li et al., 2022; Sang et al., 2022; Xu et al., 2023a; Li L. et al., 2024; Ju et al., 2025). China's CBM resources are widely distributed in the Carboniferous-Permian coal-bearing basins such as the Ordos, Qinshui, and Sichuan Basins, as well as the Jurassic-Cretaceous coal-bearing basins including the Junggar, Tarim, Turpan-Hami, Erlian, Hailar, and Sanjiang Basins (Zou et al., 2019). In recent years, a series of major breakthroughs have been achieved in deep CBM (burial depth more than 2000 m) exploration and development in the eastern margin of Ordos Basin, and significant progress has been made in some regions such as Daning-Jixian, Shenfu, Daniudi, and Yulin, collectively driving the basin's annual CBM production to exceed 1.1×10^{10} m^3 (Guo et al., 2022; Li Y. et al., 2023; Li Y. et al., 2024; Xu et al., 2023b; Xu et al., 2024). These examples have shattered the burial depth barrier for CBM exploration and development, significantly advancing prospective research and risk exploration of deep CBM in China. They have also clarified the reservoir formation characteristics of deep CBM, dominated by "high-to-over saturation, low water content, high stress, and ultra-low permeability", along with its immense resource development potential (Li S. et al., 2023; Qin, 2023).

Currently, deep CBM has become a key field for increasing reserves and production of unconventional natural gas in China. The unconventional natural gas can hold significant importance for ensuring national energy security and supporting the achievement of the "carbon peak and carbon neutrality" goals (Chen et al., 2023; Luo and Zhu, 2023; Zhang et al., 2025). Preliminary exploratory research also indicates that the composition, abundance, type, and maturity of organic matter are fundamental factors determining the gas generation capacity of coal-bearing strata (Shao et al., 2017; Qu et al., 2021; Wang et al., 2022; Li G. et al., 2025). However, different sedimentary environments in coal-bearing strata result in variations in the composition, content, type, and maturity of organic matter. These variations consequently impact the gas generation capacity and resource potential of CBM. Therefore, investigating the correlation between the sedimentary environment of coal-bearing strata and organic matter enrichment is fundamental for evaluating deep CBM resources.

The Sichuan Basin is a typical superimposed petroliferous basin in China. The Late Permian Longtan Period represents the primary coal-forming stage as a major hydrocarbon-producing unit, with widely distributed coal-bearing strata belonging to typical coastal tidal flat-lagoon facies within a marine-continental transitional depositional system (Zhang et al., 1993; Borjigen et al., 2014; Lin et al., 2018; Ming et al., 2024; Xie et al., 2024). The total thickness of the Longtan Formation coal-bearing strata ranges from approximately 60–160 m. It is primarily composed of dark gray to gray-black mudstone/shale, siltstone, and sandstone interbedded with multiple coal seams and limestone layers, and the coal seams are thin but numerous, exhibiting favorable prospects for deep CBM exploration and development (Wen et al., 2024a; Wen et al., 2024b; Wang et al., 2025). The type of organic matter in the coal-bearing strata is primarily by III-Type kerogen (sapropelic type), and the vitrinite reflectance is generally greater than 2%, indicating a higher gas-generating capacity. Presently, CBM exploration and development within the 2000 m burial depth range at the margins of the Sichuan Basin are relatively advanced. Some wells such as CGC1 Well, SD1 Well, and Y2 Well, have achieved significant breakthroughs in the exploration assessment and utilization of CBM (Bi et al., 2018; Deng et al., 2022; He et al., 2025). However, the interior of the Sichuan Basin still lacks deep CBM exploration wells, and measured geological data is insufficient. This deficiency has resulted in limited research on the correlation between sedimentary environment and organic matter enrichment in the coal-bearing strata, severely constraining the progress of deep CBM exploration and development in this region. NT1H Well is a risk exploration well of deep CBM deployed by PetroChina Southwest Oil and Gas Field Company in the interior of the Sichuan Basin. It was completed in March 2024, and the burial depth of the Longtan Formation exceeded 4000 m. This well will better reveal the CBM reservoir characteristics in central Sichuan Basin, understand the dynamic changes of CBM under high-temperature and high-pressure conditions, and indicate the enrichment mechanisms of deep CBM, thereby advancing the exploration and development process in this region. Based on the petrological and geochemical analysis of core samples from the coal-bearing strata of the Longtan Formation in NT1H Well, this study aims to investigate the correlation between the sedimentary environment and organic matter enrichment (the component, abundance, and maturity of organic matter) and reveal the organic matter enrichment mechanism in the coal-bearing strata and its primary constrained conditions.

2 Geological setting

Based on the current development degree of fault-fold structures in the Sichuan Basin (Tong, 2000; Liu et al., 2021), the region can be broadly divided into the following zones:

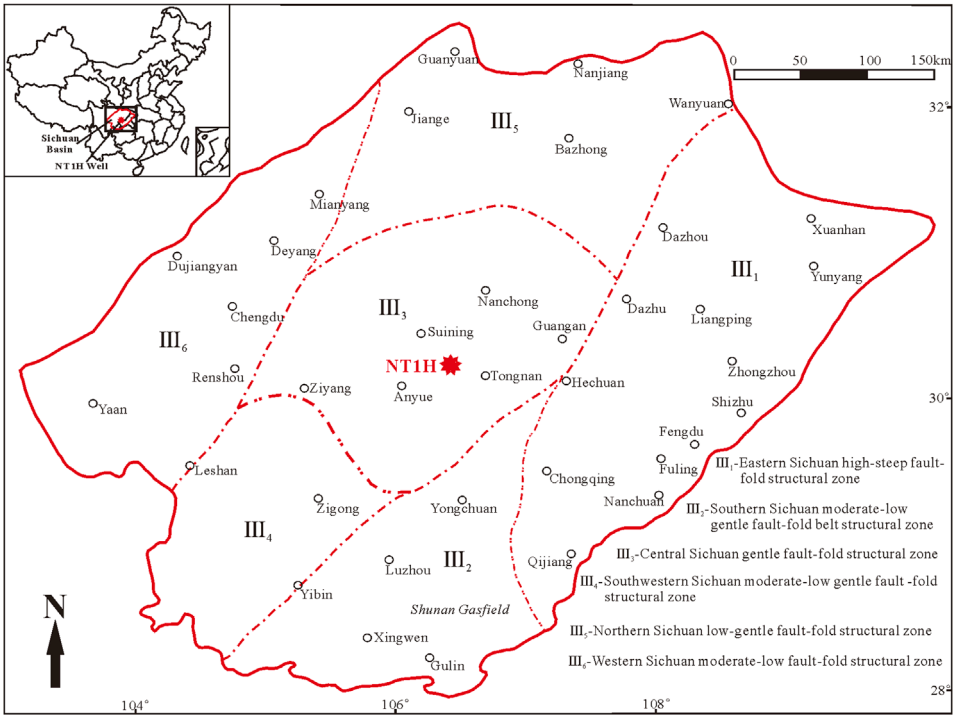

FIGURE 1
The fault-fold structures of the Sichuan Basin and the structural position of NT1H Well.

the Eastern Sichuan High-Steep Fault-Fold Structural Zone, the Southern Sichuan Moderate-Low Gentle Fault-Fold Structural Zone, the Southwestern Sichuan Moderate-Low Gentle Fault-Fold Structural Zone, the Central Sichuan Gentle Fault-Fold Structural Zone, the Northern Sichuan Low-Gentle Fault-Fold Structural Zone, and the Western Sichuan Moderate-Low Gentle Fault-Fold Structural Zone (Figure 1). Among these, the Eastern Sichuan, Southern Sichuan, and Central Sichuan regions generally represent the three levels of structural development within the basin. The Central Sichuan region constitutes a stable remnant block of the Yangtze Platform, characterized by a large monoclinal structure dipping northwestward, upon which extremely gentle NE-trending and NW-trending anticlines and nosing structures have developed, exhibiting an extremely low degree of fault-fold structure development. The Dongwu tectonic movement and the Emeishan mantle plume activity event in the late Middle Permian triggered tectonic-sedimentary differentiation of the early Late Permian (Longtanian/Wujiapingian) in the Sichuan Basin (He et al., 2021; Yuan et al., 2025). This further accentuated the basin's paleogeomorphological pattern of higher elevation in the south and lower elevation in the north, leading to the sequential development from the southwestern to the northeastern basin of the Emeishan Basalt, the continental Xuanwei Formation, the transitional Longtan Formation, and the marine Wujiaping Formation.

NT1H Well, which encountered the Longtan Formation, is located in the Moxi structure of the Leshan-Longnvsi paleo-uplift in central Sichuan Basin (Wen et al., 2024a; Wen et al., 2024b). The Leshan-Longnvsi paleo-uplift is a gigantic nose-shaped paleo-uplift formed during the Caledonian period and has the characteristics of large scale, long-term development and inheritance. Influenced by the Tongwan and Caledonian movements, the strata below the Permian have undergone varying degrees of erosion or are missing. In NT1H Well, the Longtan Formation has a burial depth ranging from 4224 to 4382 m, with a cumulative coal seam thickness exceeding 10 m (Figure 2). The Upper Permian Longtan Formation in the well consists predominantly of dark gray to gray-black mudstone/shale and siltstone, interbedded with multiple thin coal seams, representing a coastal tidal flat-lagoon depositional system within a marine-continental transitional setting. It exhibits an unconformable contact with the underlying micritic bioclastic limestone of the Middle Permian Maokou Formation and a conformable contact with the overlying micritic limestone and mudstone/shale of the Upper Permian Changxing Formation. The Longtan Formation can be divided into upper, middle, and lower members based on well logging curves, sequence stratigraphy, and lithological characteristics (Ming et al., 2024; Wen et al., 2024a; Wen et al., 2024b; Wang et al., 2025). The upper member is primarily composed of limestone, sandstone, and mudstone, and the coal seams are undeveloped. The middle member is dominated by silty mudstone, muddy siltstone-sandstone, and mudstone/shale, interbedded with multiple thin coal seams (e.g., the fourth to ninth coal seams). The immediate roof and floor of the coal seams are predominantly carbonaceous mudstone/shale. The lower member is mainly composed of mudstone/shale, silty mudstone, and tuffaceous-muddy siltstone-sandstone, interbedded with 3 sets of thin coal seams (e.g., the first to third coal seams). Therefore, the coal-bearing strata in the NT1H

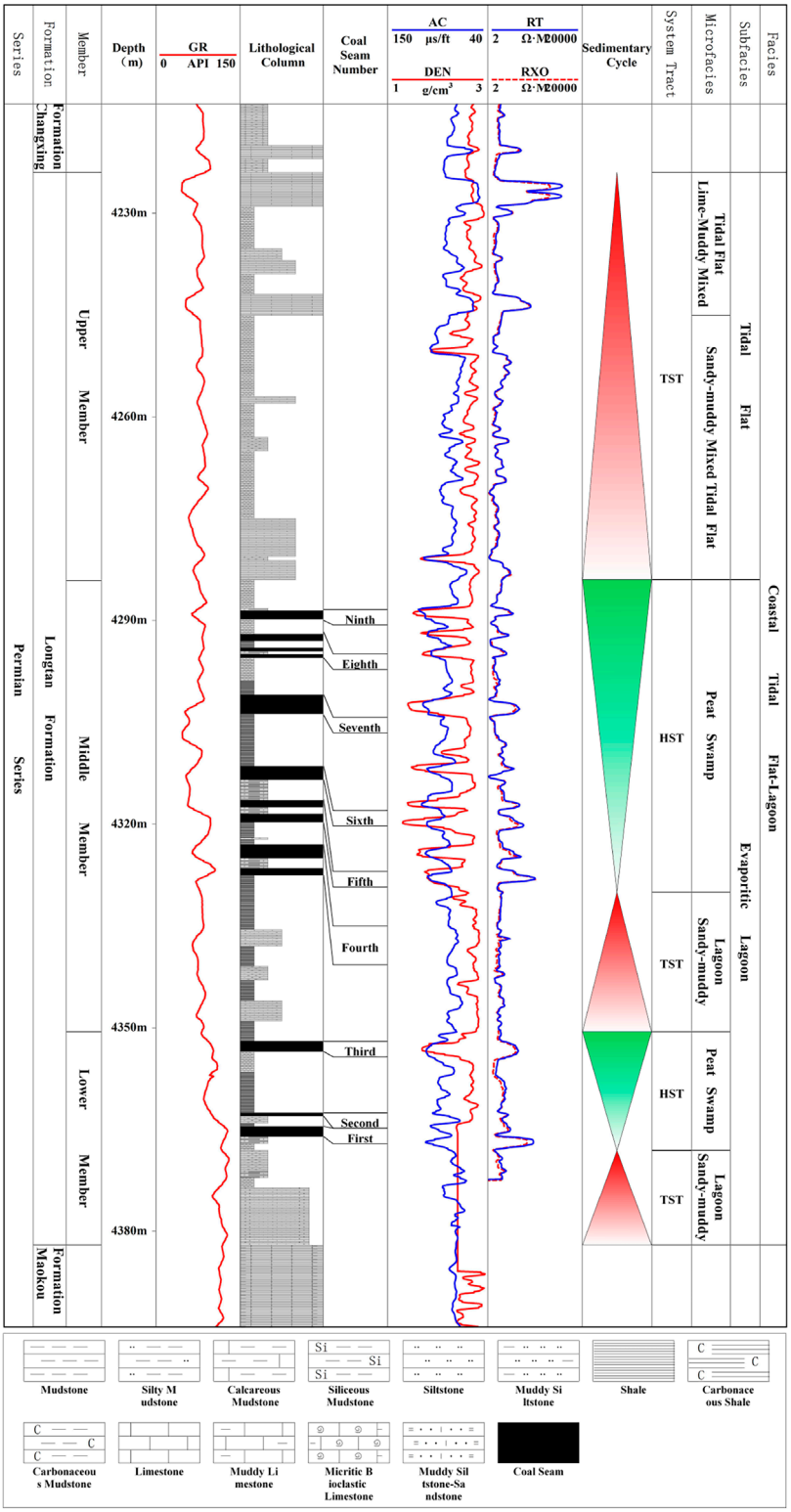

FIGURE 2
The stratigraphic column of the Upper Permian Longtan Formation in NT1H Well.

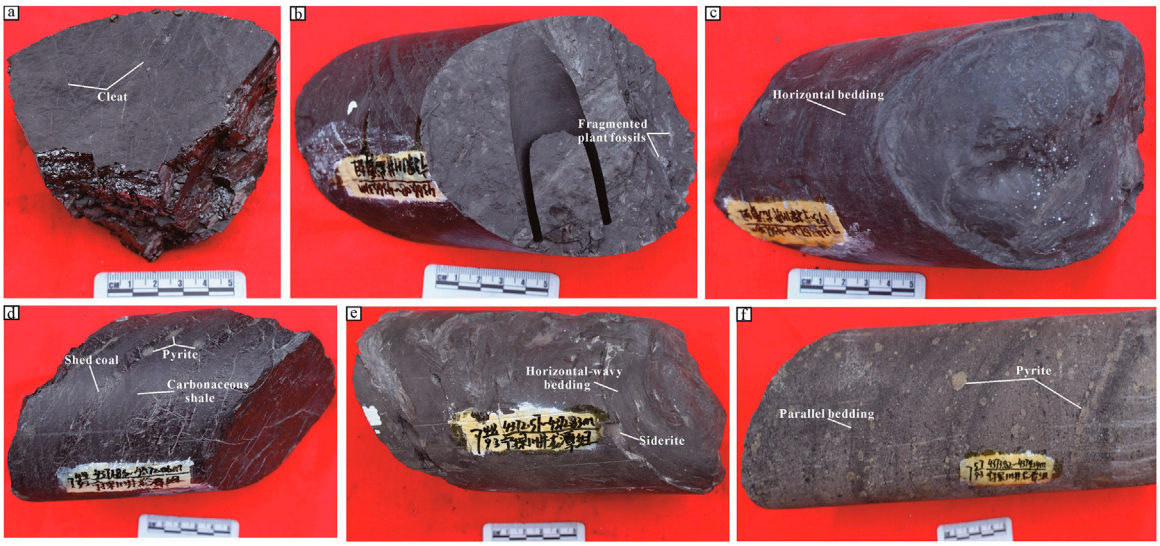

FIGURE 3
Typical macroscopic lithological photographs of the lower Longtan Formation in NT1H Well. **(a)** First coal seam, 4365.5–4365.59 m; **(b)** Carbonaceous shale, 4366.08–4366.33 m; **(c)** Mudstone, 4367.20–4367.38 m; **(d)** Carbonaceous shale interbedded with multiple shed coals less than 1 cm, 4371.86–4372.06 m; **(e)** Silty mudstone, 4372.57–4372.83 m; **(f)** Muddy siltstone-sandstone, 4373.82–4374.14 m.

Well are primarily developed within the middle-lower Longtan Formation.

3 Materials and methods

All the materials in this study were from 59.5 m of drill cores (three burial depth ranges of 4284–4305.2 m, 4316–4338 m, and 4365.5–4381.8 m) in the middle-lower coal-bearing Longtan Formation of NT1H Well, Sichuan Basin (Figures 1, 2). For observations and tests, a total of 85 well-core samples were collected from the target interval of coal-bearing strata in the middle-lower member of the Longtan Formation, including shale, mudstone, muddy siltstone, silty mudstone, and coal rocks. This study selected 24 samples for thin section preparation and identification, 15 samples for whole-rock X-ray diffraction (XRD) analysis, 8 samples for field emission scanning electron microscopy (FE-SEM) observation, 4 samples for trace element determination, 20 samples for the content testing of total organic carbon (TOC), 8 samples for vitrinite reflectance (Ro) measurement, and 6 samples for maceral analysis. The burial depth of collected core samples was finally recorded by the average value. All the data was measured in the laboratory of the Chongqing Mineral Resources Supervision and Testing Center (Chinese Ministry of Land and Resources) and the laboratory of Wuhan Xinshengji Technology Co., Ltd.

Mineralogical characteristics and lithological compositional variations were assessed using thin sections, XRD analysis, trace elements, and FE-SEM. Thin sections were prepared at a thickness of 0.03 mm, and observations were made using a polarizing Zeiss microscope (Axio Scope A1). XRD analyses were performed using a Germany Bruker D8 advance X-ray Diffractometer. The analytical method referred to the Chinese oil and gas industry standard of SY/T 5163–2018 [Analysis method for clay minerals and ordinary non-clay minerals in sedimentary rocks by the X-ray diffraction]. Trace element content, with a certain unit of parts per million (ppm), was determined using a Thermo Scientific MAT 253 Inductively Coupled Plasma Mass Spectrometry (ICP-MS). FE-SEM observation was conducted using a Germany Zeiss Gemini SEM 500, and the test standard referred to the Chinese oil and gas industry standard of SY/T 5162–2021 [Analytical method for rock samples by scanning electron microscope]. The degree of organic matter enrichment was identified by TOC contents, Ro, and maceral. TOC was measured using a Germany Multi N/C detector, and the measurement was carried out in accordance with the national standard of GB/T 19145–2022 [Determination for total organic carbon in sedimentary rock]. Macerals and Ro were mainly measured using a Leica DM4500P light microscope (Leica, Wetzlar, Germany) with a ×40 objective to analyze the volume percentages of macerals and evaluate the thermal maturity of organic matter based on reflectance spectrometry, fluorescence, and transmission spectrometry. The analytical methods of maceral referred to the national standard of GB/T 8899–2013 [Determination of maceral group composition and minerals in coal], and the Chinese oil and gas industry standard of SY/T 6414–2014 [Maceral identification and statistical methods on polished surfaces of whole rocks]. The Ro program was conducted by the national standard of GB/T 6948–2008 [Method of determining microscopically the reflectance of vitrinite in coal], and the Chinese oil and gas industry standard of SY/T 5124–2012 [Method of determining microscopically the reflectance of vitrinite in sedimentary]. Five thermal evolution stages could be generally identified, i.e., immature stage (Ro < 0.5%), lowly mature stage (Ro, 0.5 %–0.7%), mature stage (Ro, 0.7 %–1.3%), highly mature stage (Ro, 1.3 %–2.0%), and overmature stage (Ro > 2.0%).

FIGURE 4
Representative macroscopic lithological photographs of the middle Longtan Formation in NT1H Well. **(a)** Mudstone, 4284.69–4284.87 m; **(b)** Ninth coal seam and its immediate roof carbonaceous shale, 4288.38–4288.54 m; **(c)** Mudstone, 4290.37–4290.55 m; **(d)** Mudstone, 4295.10–4295.30 m; **(e,f)** Seventh coal seam, 4301.28–4301.36 m and 4303.48–4303.59 m; **(g)** Shale, 4304.59–4304.72 m; **(h,i)** Fourth coal seam, 4324.48–4324.65 m; **(j)** Carbonaceous shale, 4324.91–4325.12 m; **(k)** Shale, 4332.74–4332.94 m; **(l)** Muddy siltstone-sandstone, 4336.92–4337.23 m.

4 Results and discussion

4.1 Petrologic features of the coal-bearing strata

Through core observation, thin section identification under polarized microscopy, FE-SEM, whole-rock mineral composition analysis, and trace element determination of the coal-bearing strata in the middle-lower Longtan Formation of NT1H Well, the representative core samples are selected for detailed characterization as follows.

4.1.1 Macroscopic and microscopic lithological characterization

The macro- and micro-scale sedimentary structures, lithology, and grain size variations observed in core samples of NT1H Well serve as critical indicators for determining sedimentary

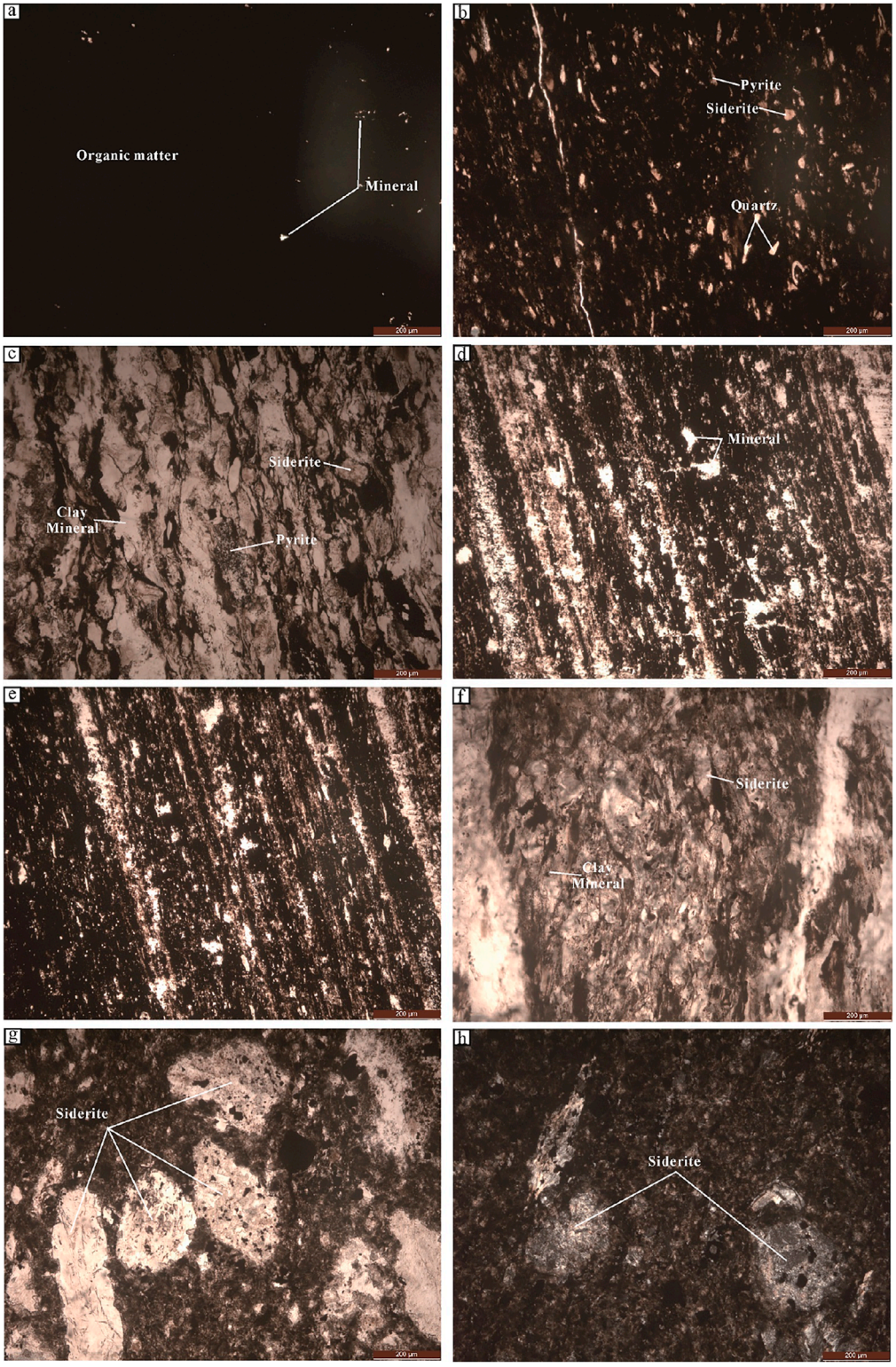

FIGURE 5
Typical microscopic lithological photographs of the lower Longtan Formation in NT1H Well. **(a)** First coal seam, 4365.59 m; **(b)** Mudstone, 4367.38 m; **(c)** Muddy siltstone-silty mudstone, 4368.59 m; **(d,e)** Carbonaceous mudstone/shale, horizontally-laminated bed less than 20um alternating light and dark, 4371.86 m; **(f)** Tuffaceous-silty mudstone, 4373.38 m; **(g,h)** Muddy siltstone-sandstone with numerous siderite nodules, 4374.74 m.

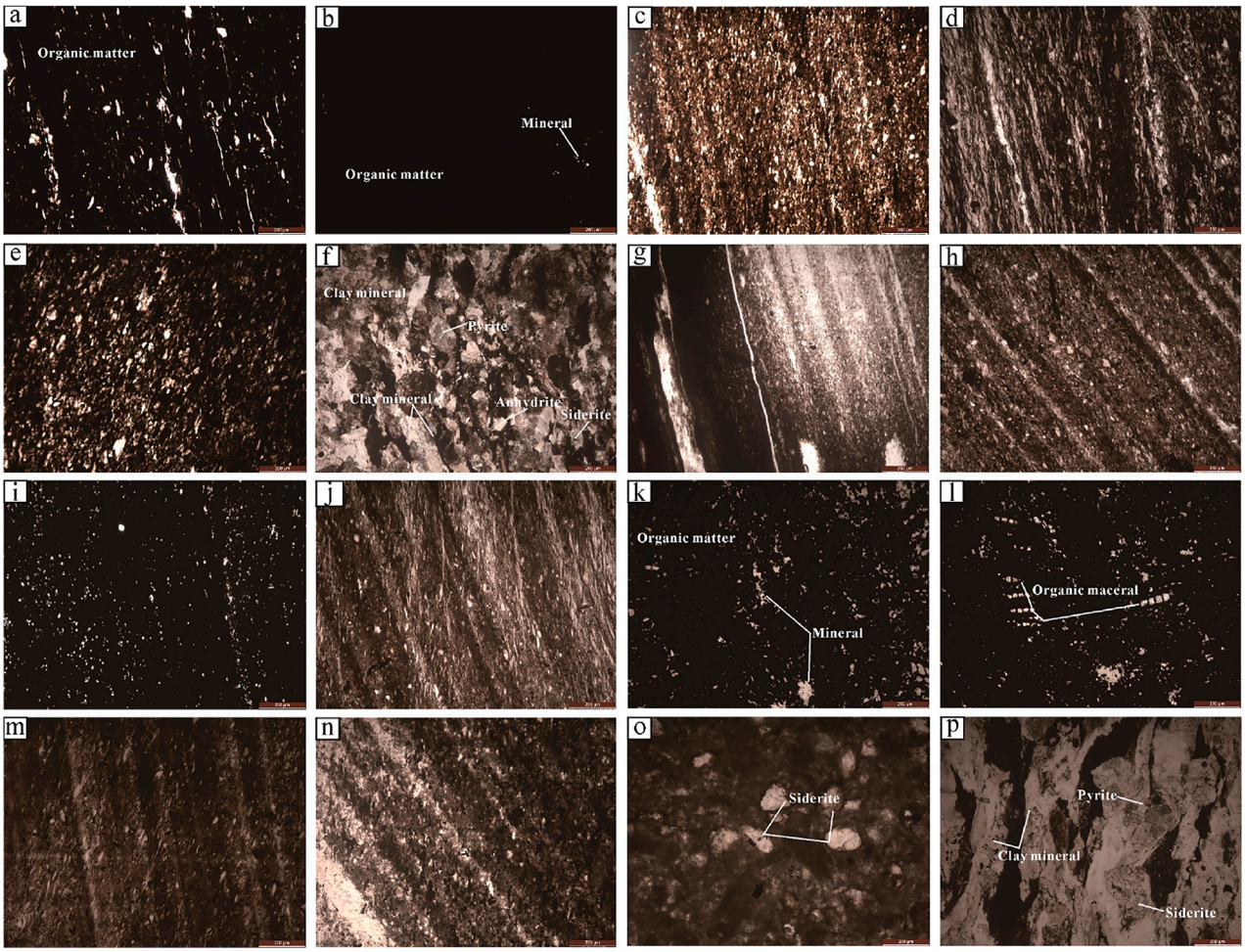

FIGURE 6
Representative microscopic lithological photographs of the middle Longtan Formation in NT1H Well. **(a)** Carbonaceous mudstone/shale, 4287.8 m; **(b)** Ninth coal seam, 4288.62 m; **(c)** Silty mudstone/shale, horizontally-laminated bed less than 20um, 4291.91 m; **(d)** Mudstone/shale, horizontal-wavy laminated bed less than 20um, 4294.58 m; **(e)** Silty mudstone, 4296.48 m; **(f)** Tuffaceous-muddy siltstone, 4298. 83 m; **(g)** Mudstone/shale, 4304.72 m; **(h)** Mudstone/shale, horizontally-laminated bed less than 20 um alternating light and dark, 4317.45 m; **(i)** Carbonaceous mudstone/shale, 4319.02 m; **(j)** Mudstone/shale, horizontal-wavy laminated bed less than 20 um alternating light and dark, 4320.27 m; **(k,l)** Fourth coal seam, 4326.37 m; **(m)** Mudstone/shale, horizontally-laminated bed alternating light and dark, 4327.8 m; **(n)** Mudstone/shale, horizontally-laminated bed alternating light and dark, 4331.13 m; **(o)** Tuffaceous-muddy siltstone-sandstone with numerous siderite nodules, 4336.23 m; **(p)** Tuffaceous-muddy siltstone-sandstone, 4337.55 m.

environment and organic matter enrichment. In the middle-lower Longtan Formation, the coal-bearing strata primarily consist of tuffaceous-muddy siltstone-sandstone, silty mudstone, carbonaceous shale, and mudstone/shale interbedded with multiple thin coal seams (Figures 2–7). Vertically, the rock grain size exhibits variability, but the normal and reverse grading rhythms are poorly developed. The mudstones/shales lack distinctly macroscopic bedding but display well-developed laminated microstructure. The muddy siltstone-sandstone and silty mudstone show clear parallel bedding, horizontal bedding, and horizontal-wavy bedding. Taking the first and fourth coal seams as examples, the macroscopic types of coal rock are predominantly semi-bright to semi-dull coal, characterized by short cylindrical to columnar primary structures. Microscopically, in addition to enriched organic matter with abundant micropores, the two coal seams contain a certain amount of inorganic minerals. Coal cleats, the natural fracture system in coal seams, are primarily classified into face cleats and butt cleats. Face cleats are continuous, well-documented master cleats, while butt cleats are shorter and terminated at face cleats, forming an interconnected network. Well-developed cleats provide primary pathways for gas flow, significantly enhancing reservoir productivity. Conversely, poor cleat development can severely restrict gas migration, negatively impacting the reservoir's performance and economic viability. In the coal samples from NT1H Well, the coal cleats are well-developed, mostly distributed in a reticular pattern with good connectivity, and have strong storage and permeability, which favor the enrichment of free gas. The coal rock is primarily composed of organic matter, quartz, clay minerals, and small amounts of pyrite, siderite, carbonate minerals, and other minerals. On the macroscopic scale of the sample surface by SEM observation, granular quartz particles and abundant filamentous, banded, or

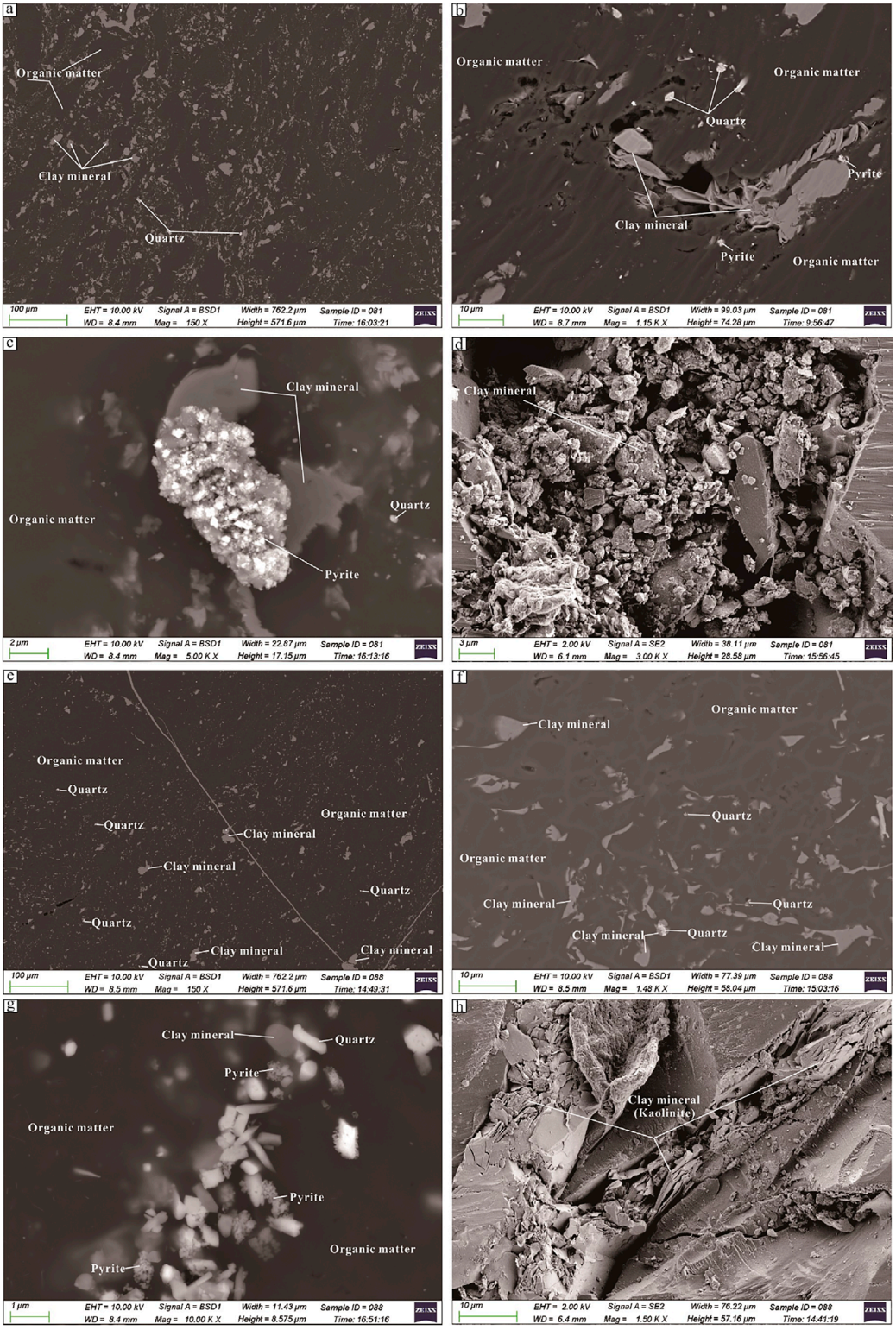

FIGURE 7
The FE-SEM photographs of the first and fourth coal seams in the middle-lower Longtan Formation of NT1H Well. **(a–d)** coal rock, fourth coal seam; **(e–h)** coal rock, first coal seam.

massive clay minerals are visible. Under higher magnification, well-developed granular and framboidal pyrite can be observed, along with well-developed pores within the organic matter. Clay seams are visible between clay minerals, and the sample surface cavities are filled predominantly with massive and flaky clay minerals, such as kaolinite.

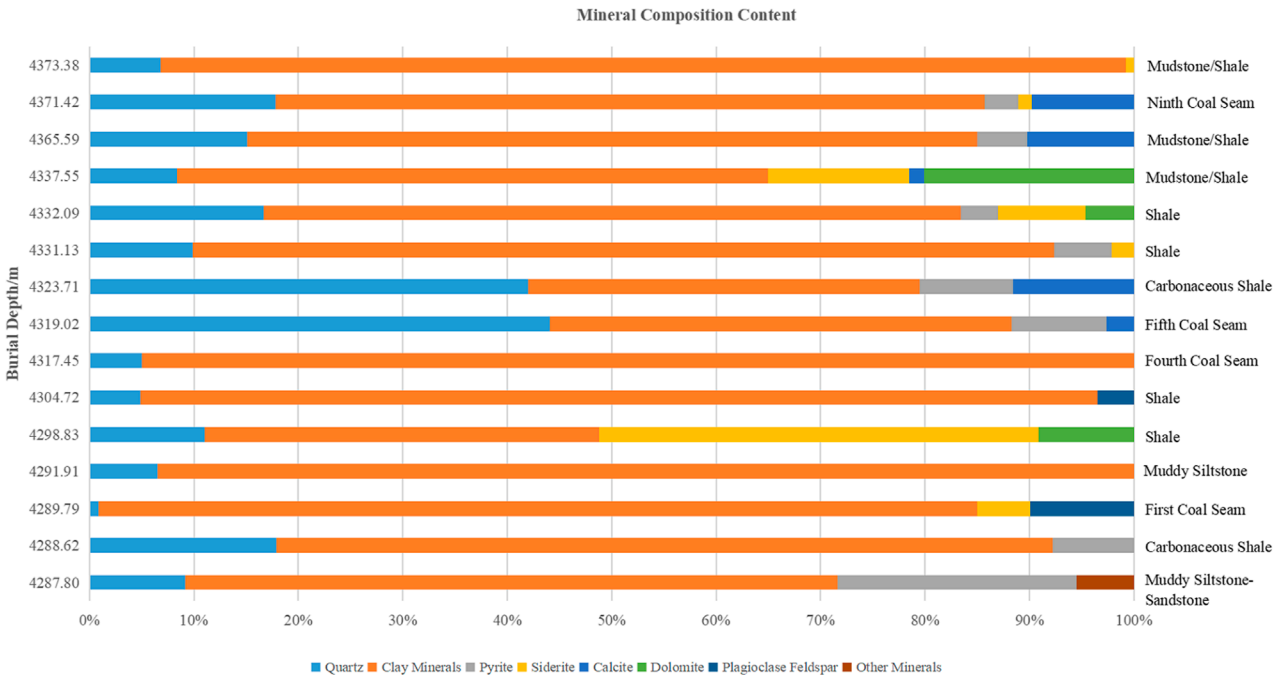

FIGURE 8
The distributional pattern on whole-rock mineral composition of different rocks in the middle-lower Longtan Formation of NT1H Well.

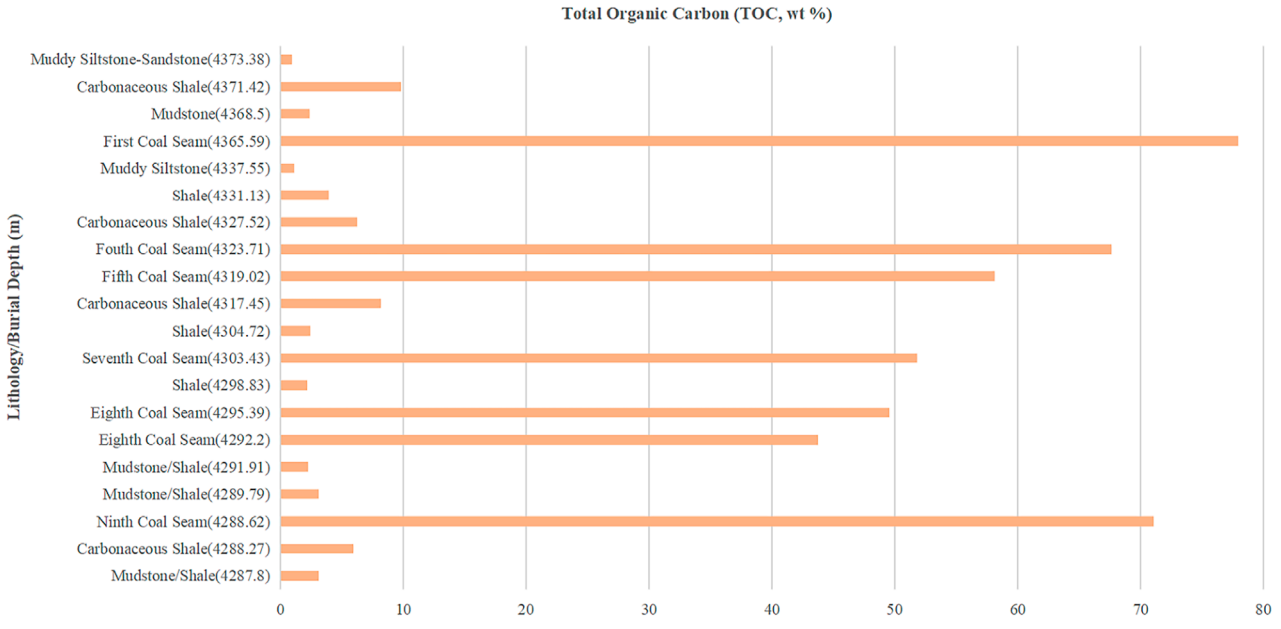

FIGURE 9
The distribution on the TOC content of different rocks in the middle-lower Longtan Formation of NT1H Well.

4.1.2 Mineral composition characterization

Whole-rock mineral quantitative analysis is conducted on 15 core samples of different rocks (Table 1; Figure 8). The results indicate that most mudstones/shales, coal rocks, muddy siltstones, and tuffaceous-muddy siltstone-sandstones are predominantly composed of quartz and clay minerals in the coal-bearing strata of the middle-lower Longtan Formation, closely associated with terrigenous clastic materials from the coastal zone. The quartz content in mudstones/shales (including mudstone/shale, shale, and carbonaceous shale) ranges from 0.9% to 17.8%, with an average of 9.1%, while the clay mineral content ranges from 37.8% to 95.0%, averaging 75.7%. In addition to abundant organic matter, coal seams

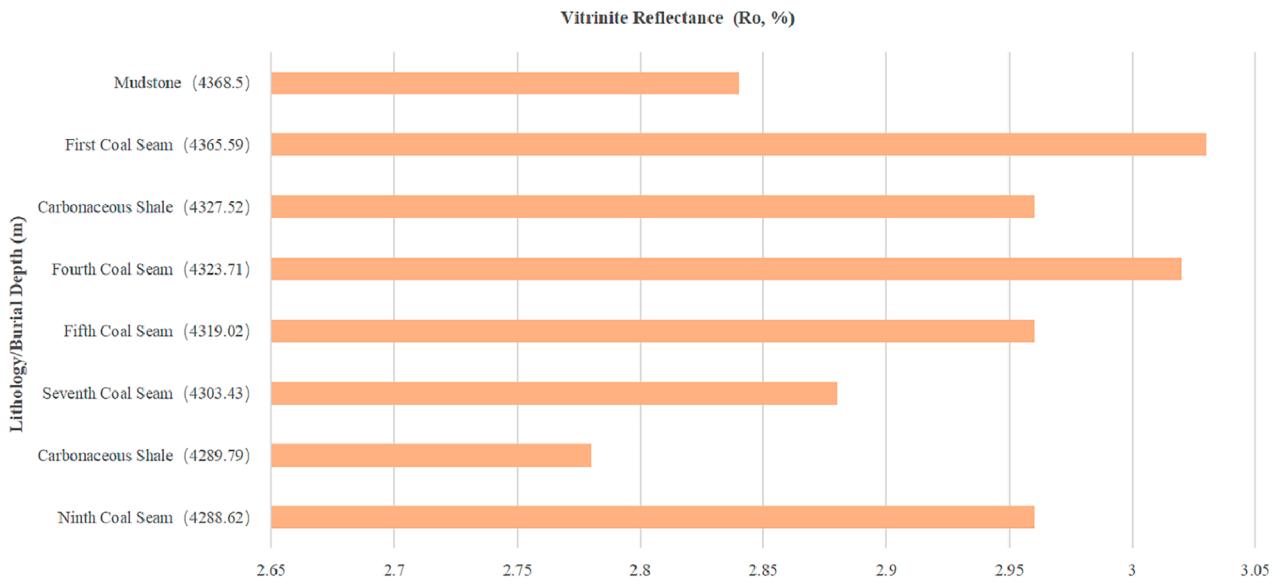

FIGURE 10
The distribution on the Ro values of coal rocks and mudstones/shales in the middle-lower Longtan Formation of NT1H Well.

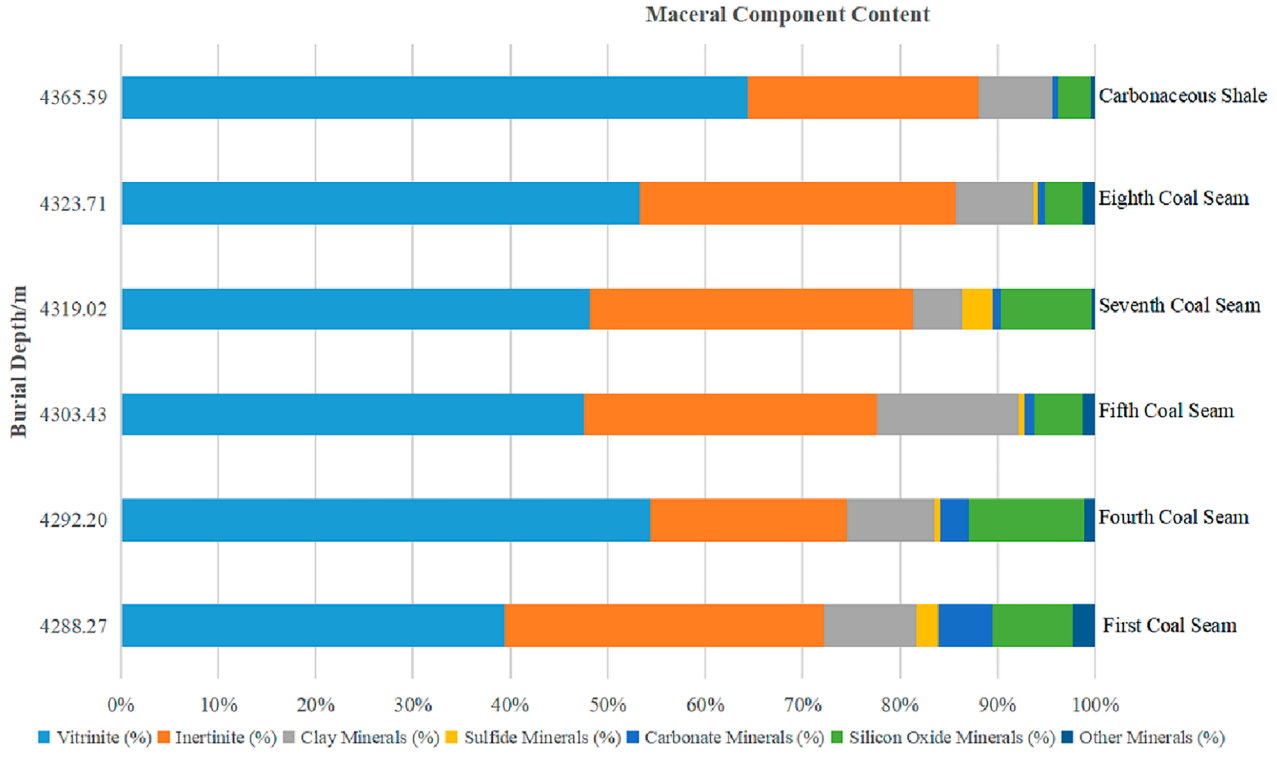

FIGURE 11
The distribution on the maceral components of major coal rocks and their immediate roofs and floors in the middle-lower Longtan Formation of NT1H Well.

also contain a certain amount of quartz and clay mineral. When calculating mineral content in coal rocks on a mineral-free basis, the coal samples from the first and ninth coal seams exhibit higher clay mineral contents of 69.9% and 74.3%. In contrast, coal samples from the fourth and fifth coal seams have the quartz contents of 42.0% and 44.1%, and the clay mineral contents of 37.5% and 44.2%. For muddy siltstone and tuffaceous-muddy siltstone-sandstone, the quartz contents range from 6.8% to 8.4%, averaging 7.6%, while the clay mineral contents vary from 56.6% to 92.4%, averaging 74.5%. Besides quartz and clay minerals in these rocks, siderite and pyrite

TABLE 1 The data on whole-rock mineral composition of different rocks in the middle-lower Longtan Formation of NT1H Well.

Well name	Lithology	Burial depth (m)	Content of mineral components (%)							Other minerals
			Quartz	Clay minerals	Pyrite	Siderite	Calcite	Dolomite	Plagioclase feldspar	
NT1H	Mudstone/Shale	4287.80	9.2	62.4	22.9					5.5
NT1H	Ninth coal seam	4288.62	17.9	74.3	7.8					
NT1H	Mudstone/Shale	4289.79	0.9	84.1		5.1			9.9	
NT1H	Mudstone/Shale	4291.91	6.5	93.5						
NT1H	Shale	4298.83	11.0	37.8		42.1		9.1		
NT1H	Shale	4304.72	4.9	91.6					3.5	
NT1H	Carbonaceous shale	4317.45	5.0	95.0						
NT1H	Fifth coal seam	4319.02	44.1	44.2	9.1		2.6			
NT1H	Fourth coal seam	4323.71	42.0	37.5	8.9		11.6			
NT1H	Shale	4331.13	9.9	82.5	5.5	2.1				
NT1H	Shale	4332.09	16.7	66.7	3.6	8.4		4.6		
NT1H	Muddy siltstone	4337.55	8.4	56.6		13.5	1.4	20.1		
NT1H	First coal seam	4365.59	15.1	69.9	4.8		10.2			
NT1H	Carbonaceous shale	4371.42	17.8	67.9	3.2	1.3	9.8			
NT1H	Muddy siltstone-sandstone	4373.38	6.8	92.4		0.8				

10.3389/feart.2025.1690793

10.3389/feart.2025.1690793

are relatively common. The presence of pyrite and siderite serves as a clear indicator of an anoxic and reducing environment in the vertical profile. The siderite content ranges from 1.3% to 42.1%, averaging 11.8%; the pyrite content varies from 3.2% to 22.9%, averaging 8.8%. Additionally, some rocks contain certain amounts of dolomite, calcite, plagioclase feldspar, and other minerals. The carbonate minerals are generally representative minerals of marine authigenic sediments and serve as indicators of paleo-marine environments. Feldspar minerals are mainly related to the direct input of terrestrial detrital materials.

4.1.3 Characteristics of trace elements in coal seams and mudstones/shales

Some geochemical proxies are valid indicators for paleo-environmental conditions. The V/Cr and Ni/Co ratios, derived from ICP-MS analysis, are standard practice for distinguishing oxic, suboxic, and anoxic conditions (Wei, 2012). Furthermore, the use of Sr/Ba or B/Ga ratios could help to more precisely delineate the salinity variations within the tidal-lagoon depositional system (Li X. et al., 2024). The geochemical analysis of trace elements in coal seams and mudstones/shales from the NT1H Well provides significant insights into the paleo-depositional conditions. The mudstone/shale samples (e.g., at 4287.80 m and 4298.83 m) exhibit relatively high concentrations of V (309–371 ppm), Cr (207–218 ppm), Ni (55.4–257 ppm), and B (76.8–94.3 ppm), along with V/Cr ratios of 1.4–1.8 and Ni/Co ratios of 1.2–1.8. These values are indicative of suboxic to anoxic depositional conditions, with moderate enrichment of biologically significant elements. In contrast, the Ninth Coal Seam sample (4288.62 m) shows markedly lower trace element concentrations (e.g., V: 16.1 ppm, Cr: 8.32 ppm, Ni: 4.9 ppm) but an elevated B/Ga ratio (9.0), suggesting a possible influence from organic matter or freshwater influx during peat accumulation. The Sr/Ba ratios across the samples are generally low (0.2–1.1), supporting a brackish depositional setting. Overall, the trace element signatures in the middle Longtan Formation reflect a whole brackish and anoxic depositional condition.

4.2 Classification of sedimentary environment on the coal-bearing strata

Based on the petrological features of the coal-bearing strata in the Permian Longtan Formation of NT1H Well (Figures 3–8), integrated with well-log responses and sequence stratigraphic features (Figure 2), this study provides a detailed discussion on the sedimentary environment for this interval.

In the earliest Wuchiapingian (Longtanian) Age of the Late Permian, A large-scale transgression occurred in the Sichuan Basin due to global sea-level rise and regional tectonic activity possibly related to crustal extension caused by the Emeishan mantle plume (e.g., Luo et al., 2014; Hou et al., 2020; Liu et al., 2023; Figure 2). A brief acknowledgment that the role of the Emeishan mantle plume in driving regression/transgression is a potential mechanism, potentially including regional tectonic activity (crustal extension and subsidence). This inundated areas previously exposed by regression or crustal uplift. Within the first transgressive systems tract (TST), the lower Longtan Formation exhibits a lithological transition from tuffaceous-muddy siltstone-sandstone to silty

TABLE 2 The trace element contents of typical coal rocks and mudstones/shales in the middle Longtan Formation of NT1H Well.

Well name	Lithology	Burial depth (m)	V (ppm)	Cr (ppm)	Co (ppm)	Ni (ppm)	Ga (ppm)	Sr (ppm)	Ba (ppm)	B (ppm)	V/Cr	Ni/Co	Sr/Ba	B/Ga
NT1H	Mudstone/Shale	4287.80	371	207	218.0	257	32.6	554	496	94.3	1.8	1.2	1.1	2.9
NT1H	Ninth coal seam	4288.62	16.1	8.32	2.52	4.9	2.91	51	85.6	26.3	1.9	2.0	0.6	9.0
NT1H	Mudstone/Shale	4288.80	28.7	21.7	10.5	22.8	2.9	64.1	283.0	9.3	1.3	2.2	0.2	3.3
NT1H	Shale	4298.83	309	218	30.8	55.4	27.5	292	265	76.8	1.4	1.8	1.1	2.8

mudstone and mudstone/shale. The mudstone/shale contains abundant fragmented plant fossils as the source of III-Type kerogen (sapropelic type). Bedding transitions from parallel bedding and horizontal wavy bedding to horizontal bedding. The mineral composition is dominated by quartz and clay minerals, with common pyrite and siderite and occasional carbonate minerals. Overall, well logs display an approximately box-shaped pattern, with vertical variations in grain size but indistinct normal or inverse grading sequences. These characteristics reflect weakening hydrodynamic energy from shallow to deep water, a relatively sufficient terrigenous supply, and strongly reducing conditions, indicating a typical transition from sandy-muddy lagoon to muddy lagoon deposition. As water depth continued to increase, reaching a maximum before slowly shallowing with minor fluctuations, the first highstand systems tract (HST) developed mudstone/shale interbedded with multiple thin coal seams. Horizontal bedding and horizontal wavy bedding are well-developed, while well logs show serrated variations. Clay minerals increase significantly, with pyrite and siderite being extremely common. This indicates even weaker hydrodynamic conditions and stronger reducing environments, representing a rapid environmental transition from muddy lagoon into peat swamp along with regional regression in the basin.

Subsequently, regional transgression and regression reappeared in the basin during the Wuchiapingian (Longtanian) and initiated another cycle of water deepening and shallowing (e.g., Zhang et al., 1993; Lin et al., 2018; Figure 2). The middle Longtan Formation developed successively from sandy-muddy lagoon to peat swamp environments upward. Its well-log responses, sequence stratigraphy, and mineral composition resemble those of the lower Longtan Formation, and the lithology transitions from muddy siltstone-sandstone to silty mudstone and mudstone/shale interbedded with multiple thin coal seams and fragmented plant fossils. Bedding is dominated by horizontal wavy and horizontal laminations, with increased coal seam frequency but reduced individual thickness, reflecting weaker hydrodynamics and stronger reduction. Therefore, the coal-bearing strata in the middle-lower Longtan Formation of NT1H Well primarily represent lagoon subfacies, subdivided into two microfacies: sandy-muddy lagoon and peat swamp (rapidly evolved from muddy lagoon). The peat swamp constitutes the most favorable sedimentary environment for developing multiple thin coal seams in the middle-lower Longtan Formation.

4.3 Enrichment characteristics of organic matters in different rocks

By analyzing the vertical variations of organic matter abundance in core samples of NT1H Well and then combining the results of Ro tests to determine the organic matter maturity, followed by using maceral analysis to obtain the organic matter components, this approach closely integrates lithology with the characteristics of organic matter enrichment, providing a basis for studying the relationship between sedimentary environment and organic matter enrichment in the coal-bearing strata of the middle-lower Longtan Formation.

4.3.1 Organic matter abundance

Organic matter abundance is a crucial material condition for the accumulation and enrichment of deep CBM, determining the scale of CBM storage space. The higher the organic matter abundance, the greater the CBM storage capacity. The organic matter abundances of different rocks are evaluated based on the TOC contents in Table 3; Figure 9.

The results indicate that the organic matter abundance of core samples generally follows a regular change: coal exhibits the highest values, followed by mudstones/shales (including carbonaceous shale, shale, mudstone, and mudstone/shale), while muddy siltstones-sandstones show relatively low values.

For the first, fourth, fifth, eighth, and ninth coal seams, their TOC contents range from 43.76 wt% to 77.97 wt%, with an average of 59.99 wt%. Among them, the first coal seam has the highest organic matter abundance, with a TOC content of 77.97 wt%. Four carbonaceous shale samples in the roofs and floors of coal seams and the other seven mudstones/shales have TOC contents between 2.16 wt% and 9.77 wt%, averaging 4.49 wt%. The TOC contents in these rocks are much higher than that of the marine organic-rich shale in the Wufeng Formation-Longmaxi Formation of the Sichuan Basin (e.g., Wang et al., 2024; Chen et al., 2025). This reveals that the above rocks can provide better material conditions for the accumulation and enrichment of deep unconventional natural gas. But muddy siltstones-sandstones exhibit low TOC contents, ranging from 0.92wt% to 1.12wt%, indicating that they are not conducive to organic matter enrichment.

4.3.2 Organic matter maturity

The organic matter maturity usually reflects the thermal evolution degree of kerogen in source rocks and is a key parameter for analyzing the hydrocarbon-generating extent. Typically, low-maturity source rocks are dominated by biogenic gas with relatively low gas production, while high-maturity source rocks primarily yield kerogen cracking gas with a high gas generation ratio. By the comprehensive use of T_{max} and Ro data, we conduct a detailed analysis of the organic matter maturity in major coal rocks and their immediate roofs and floors with higher TOC contents, as shown in Table 4; Figure 10. The results indicate that Ro mainly ranges from 2.78% to 3.03%, with an average of 2.93%. These findings suggest that the organic matter generally experiences the overmature stage (Ro>2.0%), with strong gas-generating capacity, demonstrating favorable potential for the accumulation and production of deep CBM.

4.3.3 Organic matter component

Differences in organic matter components determine the product characteristics of source rocks and also influence hydrocarbon-generating potential. A higher vitrinite content corresponds to stronger gas-generating capacity.

Coal rocks and their immediate roofs and floors with relatively higher TOC contents are selected for maceral component testing and analysis, as shown in Table 4; Figure 11. The results indicate that the coal rocks and the surrounding carbonaceous shales are dominated by organic macerals, with fewer inorganic macerals. Among the organic macerals, vitrinite is the primary component, with content ranging from 39.4% to 64.4% (average: 51.2%),

TABLE 3 The TOC contents of different rocks in the middle-lower Longtan Formation of NT1H Well.

Well name	Lithology	Burial depth (m)	Total organic carbon (TOC, wt%)
NT1H	Mudstone/Shale	4287.80	3.12
NT1H	Carbonaceous shale	4288.27	5.94
NT1H	Ninth coal seam	4288.62	71.05
NT1H	Mudstone/Shale	4289.79	3.12
NT1H	Mudstone/Shale	4291.91	2.21
NT1H	Eighth coal seam	4292.20	43.76
NT1H	Eighth coal seam	4295.39	49.56
NT1H	Shale	4298.83	2.16
NT1H	Seventh coal seam	4303.43	51.83
NT1H	Shale	4304.72	2.43
NT1H	Carbonaceous shale	4317.45	8.19
NT1H	Fifth coal seam	4319.02	58.10
NT1H	Fouth coal seam	4323.71	67.63
NT1H	Carbonaceous shale	4327.52	6.24
NT1H	Shale	4331.13	3.91
NT1H	Muddy siltstone	4337.55	1.12
NT1H	First coal seam	4365.59	77.97
NT1H	Mudstone	4368.50	2.35
NT1H	Carbonaceous shale	4371.42	9.77
NT1H	Muddy siltstone-sandstone	4373.38	0.92

TABLE 4 The Ro values of coal rocks and mudstones/shales in the middle-lower Longtan Formation of NT1H Well.

Well name	Lithology	Burial depth (m)	Vitrinite reflectance (Ro, %)	Standard deviation (S, %)
NT1H	Ninth coal seam	4288.62	2.96	0.200
NT1H	Carbonaceous shale	4289.79	2.78	0.167
NT1H	Seventh coal seam	4303.43	2.88	0.192
NT1H	Fifth coal seam	4319.02	2.96	0.183
NT1H	Fourth coal seam	4323.71	3.02	0.161
NT1H	Carbonaceous shale	4327.52	2.96	0.190
NT1H	First coal seam	4365.59	3.03	0.188
NT1H	Mudstone	4368.50	2.84	0.259

TABLE 5 The data on the maceral components of major coal rocks and their immediate roofs and floors in the middle-lower Longtan Formation of NT1H Well.

Well name	Lithology	Burial depth (m)	Vitrinite (%)	Inertinite (%)	Content of organic maceral component (%)	Clay minerals (%)	Sulfide minerals (%)	Carbonate minerals (%)	Silicon oxide minerals (%)	Other minerals (%)	Content of inorganic maceral component-mineral composition (%)
NT1H	Carbonaceous shale	4288.27	39.4	32.8	72.2	9.5	2.2	5.6	8.3	2.2	27.8
NT1H	Eighth coal seam	4292.20	54.4	20.1	74.5	9.0	0.6	3	11.8	1.1	25.5
NT1H	Seventh coal seam	4303.43	47.6	30.0	77.6	14.6	0.6	1.0	5.0	1.2	22.4
NT1H	Fifth coal seam	4319.02	48.2	33.2	81.4	5.0	3.1	0.8	9.4	0.3	18.6
NT1H	Fourth coal seam	4323.71	53.3	32.4	85.7	8.0	0.4	0.8	3.9	1.2	14.3
NT1H	First coal seam	4365.59	64.4	23.7	88.1	7.5	0	0.6	3.4	0.4	11.9

10.3389/feart.2025.1690793

followed by inertinite at 20.1 %–33.2%, (average: 28.7%), while liptinite is absent. The first coal seam has the highest organic maceral content at 88.1%. Inorganic macerals range from 11.9 % to 27.8% (average: 20.1%), primarily consisting of clay minerals (5.0 %–14.6%), sulfide minerals (0 %–3.1%), carbonate minerals (0.6 %–5.6%), and silicon oxide minerals (3.4 %–11.8%). The first and fourth coal seams have relatively low mineral contents of 11.9% and 14.3%, whereas the seventh and eighth coal seams show increased mineral contents of 22.4% and 25.5%, with the immediate roof carbonaceous shale of the ninth coal seam being the highest (27.8%). This primarily illustrates that from the lower coal seams to the upper coal seams in the middle-lower Longtan Formation, the coal-forming environment gradually transitioned from a relatively stable, anoxic, and water-covered swamp with minimal clastic input to a dry or turbulent swamp characterized by increased hydrodynamic intensity and closer proximity to clastic source areas.

4.4 The control of sedimentary environment on organic matter enrichment in the coal-bearing strata

The organic matter enrichment in the coal-bearing strata of the middle-lower Permian Longtan Formation is profoundly influenced by the sedimentary environment, which governs both the supply and preservation of organic matter. Based on the petrological, mineralogical, and organic geochemical characteristics observed in the NT1H Well (Figures 3–11; Tables 1–5; Wen et al., 2024a; Wen et al., 2024b), the depositional setting evolved through distinct phases of transgression and regression, resulting in cyclic changes in hydrodynamic conditions, redox states, and terrigenous input. These factors collectively controlled the accumulation and preservation of organic matter.

During the initial transgressive phase (lower Longtan Formation, TST), the depositional environment transitioned from a sandy-muddy lagoon to a short-lived muddy lagoon. The presence of parallel bedding, horizontal-wavy bedding, and increasing clay mineral content up-section indicated a gradual reduction in hydrodynamic energy. The common occurrence of pyrite and siderite, along with the absence of well-developed grading sequences, suggested deposition under anoxic and reducing conditions. These conditions were conducive to the preservation of organic matter, as reduced hydrodynamics limit the reworking and oxidation of organic debris. The high terrestrial input, evidenced by quartz and clay minerals, supplied abundant plant-derived organic matter (III-type kerogen), which accumulated in the oxygen-depleted bottom waters. This resulted in mudstones/shales with moderate to high TOC contents (average 4.49 wt%), indicating effective organic matter preservation under these conditions. With continued transgression and subsequent regression (lower Longtan Formation, HST), the environment shifted rapidly from a short-lived muddy lagoon to a stable peat swamp. This transition was marked by the interbedding of mudstones/shales with thin coal seams, increased frequency of horizontal and wavy bedding, and a significant rise in clay mineral and pyrite contents. The serrated well-log patterns reflected frequent alterations between reducing muddy sediments and organic-rich peat deposits. The strongly anoxic and reducing conditions, evidenced by abundant pyrite and siderite, enhanced organic matter preservation by limiting biodegradation. Consequently, multiple thin coal seams with high TOC contents (average 59.99 wt%) developed, with the first coal seam reaching up to 77.97 wt%. The low mineral contents in the lower coal seams (e.g., first and fourth seams) further indicated minimal clastic input and a stable, waterlogged swamp environment, ideal for organic accumulation.

The second transgressive-regressive cycle occurred in the middle Longtan Formation, repeating the environmental transition from sandy-muddy lagoon to peat swamp. In this interval, hydrodynamics were much weaker and reducing conditions were much stronger than those in the lower Longtan Formation. In addition, the increasing mineral contents upwards provided direct evidence for the evolving proximity to clastic source areas. This could lead to higher coal seam frequency but reduced thickness, but the controlled mechanism on organic enrichment remained similar. The persistent anoxia and limited turbulence allowed for substantial organic matter preservation, even as increased clastic input in the upper seams (e.g., seventh and eighth coal seams) slightly diluted organic content.

4.5 Implications for deep CBM accumulation in central Sichuan Basin

The III-type kerogen, high organic matter abundance, overmature thermal evolution (Ro, average 2.93%), and dominant gas-prone macerals (vitrinite, average 51.2%) demonstrate significant potential for deep CBM generation in central Sichuan Basin. The anoxic and reducing sedimentary environments, such as sandy-muddy lagoons and peat swamps, promote the accumulation and preservation of organic matter, while the subsequent deep burial and tectonic-hydrothermal activity led to high thermal maturity. The well-developed coal cleats and organic pores observed in the coal seams are also equally critical. Particularly in the lower Longtan Formation, better reservoir properties (i.e., porosity, permeability, and pore structures) are very favorable for free gas accumulation. The vertical heterogeneity in sedimentary microfacies, however, may result in compartmentalization of gas reservoirs, with the thickest and most organic-rich coal seams (e.g., the first coal seam) likely serving as the most productive zones. Overall, the cyclic changes on sedimentary environment in the coal-bearing Longtan Formation created a series of vertically stacked, organic-rich units with strong gas generation potential. The peat swamp microfacies, in particular, represents the most favorable depositional environment for organic matter enrichment and subsequent CBM accumulation in central Sichuan Basin.

5 Conclusion

1. The coal-bearing strata in the middle-lower Longtan Formation of NT1H Well primarily consists of mudstone/shale, silty mudstone, and tuffaceous-muddy siltstone-sandstone interbedded with multiple thin coal seams. Horizontal bedding, horizontal wavy bedding, and parallel bedding are well-developed. The mineral composition is

dominated by quartz and clay minerals, with pyrite and siderite being relatively common.

2. In the middle-lower Longtan Formation of NT1H Well, the organic matter abundance in coal seams is significantly higher than that in their immediate roof and floor carbonaceous shale, as well as mudstone/shale and muddy siltstone-sandstone. The TOC contents of coal seams range from 43.76 to 77.97 wt%, with R_0 generally exceeding 2.5%, and the dominant maceral is vitrinite. Coal seams and their surrounding mudstones/shales exhibit high organic matter enrichment and strong gas-generating capacity, while muddy siltstone-sandstones have relatively lower organic matter abundance and are unfavorable for organic matter accumulation.
3. The sedimentary environment of the coal-bearing strata is mainly lagoon subfacies, including sandy-muddy lagoon and peat swamp microfacies. The peat swamp evolves from muddy lagoon deposits and is the most favorable for the organic matter enrichment in coal seams and mudstones/shales, providing a strong material basis for CBM accumulation.
4. Except for the supply of terrestrial materials, hydrodynamic and redox conditions are key controlling factors for organic matter enrichment in the coal-bearing strata of the middle-lower Longtan Formation from NT1H Well. In the peat swamp microfacies, weak hydrodynamics and a strongly reducing environment promote exceptionally high organic matter enrichment, whereas in the sandy-muddy lagoon, relatively stronger hydrodynamics and weaker reducibility lead to comparatively lower enrichment.

Data availability statement

The original contributions presented in the study are included in the article/supplementary material, further inquiries can be directed to the corresponding authors.

Author contributions

YY: Conceptualization, Supervision, Funding acquisition, Writing – original draft. XT: Writing – review and editing, Writing – original draft. ML: Formal Analysis, Writing – original draft, Methodology, Investigation, Data curation. YL: Formal Analysis, Data curation, Methodology, Writing – original draft, Investigation. JP: Writing – original draft, Investigation, Methodology, Formal Analysis, Data curation. DG: Methodology, Data curation, Writing – original draft. YeZ: Data curation, Writing – original draft, Methodology. YuZ: Writing – original draft, Data curation, Methodology. CT: Writing – original draft, Data curation, Methodology. DC: Writing – original draft, Funding acquisition, Supervision, Writing – review and editing. CC: Formal Analysis, Investigation, Writing – original draft. JW: Writing – original draft, Funding acquisition, Writing – review and editing, Supervision. TH: Formal Analysis, Investigation, Writing – original draft.

Funding

The authors declare that financial support was received for the research and/or publication of this article. This study was supported by the horizontal project from Chongqing Gas Field, PetroChina Southwest Oil and Gas Field Company (XNS Chongqing Gas Field JS 2024-20) and the project of Rolling Evaluation and Transfer Preparation of Oil and Gas Mining Right Withdrawal Blocks in Chongqing City from Chongqing planning and Natural Resources Bureau (KG1024Y101603G).

Acknowledgements

We would like to thank Guest Editor Prof. Li Ang and three reviewers for their valuable comments and constructive suggestions that help to improve the original quality of this paper.

Conflict of interest

Authors YY, YL, and CT were employed by Chongqing Gas Field, PetroChina Southwest Oil and Gas Field Company. Authors XT, JP, DG, YuZ, and DC were employed by Chongqing Huadi Resources and Environment Technology Co., Ltd. Author CC was employed by Sichuan Energy Investment Oil and Gas Exploration and Development Co., Ltd.

The remaining authors declare that the research was conducted in the absence of any commercial or financial relationships that could be construed as a potential conflict of interest.

The authors declare that this study received funding from PetroChina Southwest Oil and Gas Field Company. The funder had the following involvement in the study: study design, data collection and analysis.

Generative AI statement

The authors declare that no Generative AI was used in the creation of this manuscript.

Any alternative text (alt text) provided alongside figures in this article has been generated by Frontiers with the support of artificial intelligence and reasonable efforts have been made to ensure accuracy, including review by the authors wherever possible. If you identify any issues, please contact us.

Publisher's note

References

Bi, C. X., Shan, Y. S., Zhu, H. Y., Zhang, J. Q., Hu, Z. F., Su, S. C., et al. (2018). Industrial gas production of CBM obtained by well CGC1 in southern sichuan. *Geol. China* 45 (5), 1976–1077. (in Chinese).

Borjigen, T., Qin, J. Z., Fu, X. D., Yang, Y. F., and Lu, L. F. (2014). Marine hydrocarbon source rocks of the Upper Permian longtan formation and their contribution to gas accumulation in the northeastern sichuan basin, southwest China. *Mar. Petroleum Geol.* 57, 160–172. doi:10.1016/j.marpetgeo.2014.05.005

Cao, D. Y., Yao, Z., and Li, J. (2014). Evaluation status and development trend of unconventional gas in coal measure. *Coal Sci. Technol.* 42 (1), 89–92. (in Chinese, with English abstract).

Chen, S. D., Tang, D. Z., Hou, W., Li, Y. Z., Tao, S., Xu, H., et al. (2023). Geological particularity and reservoir engineering response of deep coalbed methane. *Acta Pet. Sin.* 44 (11), 1993–2006. (in Chinese, with English abstract).

Chen, M. F., Yang, J. J., Lu, Z. Y., Ming, Y., Wang, H., Chen, S. Y., et al. (2025). Comparison of geological conditions and prospects of exploration potential of shale gas in upper permian Wujiaping formation and longtan formation, Sichuan Basin. *Front. Earth Sci.* 13, 1557328. doi:10.3389/feart.2025.1557328

Dai, J. X., and Gong, J. M. (2018). Establishment of coal-derived gas geological theory and its strategic significance to the development of natural gas industry in China. *China Pet. Explor.* 23 (4), 1–10. (in Chinese, with English abstract).

Deng, M., Lan, Y. F., Cheng, J. X., Wang, Z. H., Yu, Q., Liu, A. R., et al. (2022). Shale gas (CBM) potential of Longtan formation in Shihao mining area, Southeast Sichuan: a case study of well SD1. *Acta Geosci. Sin.* 43 (3), 295–308. (in Chinese, with English abstract).

Guo, X. S., Zhou, D. H., Zhao, P. R., Liu, Z. Q., Zhang, D. W., Feng, D. J., et al. (2022). Progresses and directions of unconventional natural gas exploration and development in the Carboniferous-Permian coal measure strata, ordos Basin. *Oil and Gas Geol.* 43 (5), 1013–1023. (in Chinese, with English abstract).

He, Z. L., Nie, H. K., Li, S. J., Liu, G. X., Ding, J. H., Bian, R. K., et al. (2021). Differential occurrence of shale gas in the Permian longtan Formation of upper Yangtze region constrained by plate tectonics in the Tethyan domain. *Oil and Gas Geol.* 42 (1), 1–15. (in Chinese, with English abstract).

He, X. P., Wang, K. M., Luo, W., Gao, Y. Q., Liu, N. N., Guo, T., et al. (2025). Geological characteristics and main enrichment controlling factors of coalbed methane in Nanchuan area, southeastern sichuan basin. *Petroleum Geol. and Exp.* 47 (1), 64–76. (in Chinese, with English abstract).

Hou, Z. S., Fan, J. X., Henderson, C. M., Yuan, D. X., Shen, B. H., Wu, J., et al. (2020). Dynamic palaeogeographic reconstructions of the Wuchiapingian stage (lopingian, late Permian) for the South China block. *Palaeogeogr. Palaeoclimatol. Palaeoecol.* 546, 109667. doi:10.1016/j.palaeo.2020.109667

Jamieson, M., Elson, M., Carruthers, R., and Ordens, C. M. (2020). The contribution of citizen science in managing and monitoring groundwater systems impacted by coal seam gas production:an example from the surat Basin in Australia's great artesian Basin. *Hydrogeology J.* 28 (1), 439–459. doi:10.1007/s10040-019-02050-8

Ju, W., Tao, S., Yang, Z. B., Cheng, J. Y., Shang, H. Y., Ning, W. K., et al. (2025). Current status and development trends of deep coalbed methane research in China. *Petroleum Geol. and Exp.* 47 (1), 9–16. (in Chinese, with English abstract).

Li, Y., Pan, S. P., Ning, S. Z., Shao, L. Y., Jing, Z. H., and Wang, Z. S. (2022). Coal measure metallogeny: metallogenic system and implication for resource and environment. *Sci. China Earth Sci.* 65, 1211–1228. doi:10.1007/s11430-021-9920-4

Li, S., Qin, Y., Tang, D. Z., Shen, J., Wang, J. J., and Chen, S. D. (2023). A comprehensive review of deep coalbed methane and recent developments in China. *Int. J. Coal Geol.* 279, 104369. doi:10.1016/j.coal.2023.104369

Li, Y., Gao, S., Wu, P., Xu, L. F., Feng, L. T., Hu, W. Q., et al. (2023). Evaluation and correction of prediction model for free gas content in deep coalbed methane: a case study of deep coal seams in the eastern margin of Ordos Basin. *Acta Pet. Sin.* 44 (11), 1892–1902. (in Chinese, with English abstract).

Li, L., Ma, S. M., Liu, X., Liu, J., Lu, Y., Zhao, P., et al. (2024). Coal measure gas resources matter in China: review, challenges, and perspective. *Phys. Fluids* 36 (7), 071301. doi:10.1063/5.0218328

Li, X. B., Xiao, K., Sun, L., Wu, S. H., Xu, Z. H., Jiang, S. C., et al. (2024). Paleosalinity characteristics of the 1st member in the Lower cretaceous prosopis formation, Baobab North Sag, Bongor Basin. *Front. Earth Sci.* 12, 1450001. doi:10.3389/feart.2024.1450001

Li, Y., Xu, F. Y., Tang, S. H., Wang, Y. B., Meng, S. Z., and Xu, Q. (2024). Progress and development direction of coalbed methane(coal-rock gas)exploration and development in the ordos Basin. *Nat. Gas. Ind.* 10, 63–79. (in Chinese, with English abstract).

Li, G. X., Jia, C. Z., Zhao, Q., Zhou, T. Q., and Gao, J. L. (2025). Coal-rock gas accumulation mechanism and the whole petroleum system of coal measures. *Petroleum Explor. Dev.* 52 (1), 33–49. (in Chinese, with English abstract). doi:10.1016/s1876-3804(25)60003-6

Lin, L. B., Yu, Y., Zhai, C. B., Li, Y. H., Wang, Y. N., Liu, G. X., et al. (2018). Paleogeography and shale development characteristics of the Late Permian longtan formation in southeastern Sichuan Basin, China. *Mar. Petroleum Geol.* 95, 67–81. doi:10.1016/j.marpetgeo.2018.04.016

Liu, J., Yao, Y. B., Liu, D. M., Xu, L., Elsworth, D., Huang, S. P., et al. (2018). Experimental simulation of the hydraulic fracture propagation in an anthracite coal reservoir in the southern qinshui basin, China. *J. Petroleum Sci. Eng.* 168, 400–408. doi:10.1016/j.petrol.2018.05.035

Liu, S. G., Yang, Y., Deng, B., Zhong, Y., Wen, L., Sun, W., et al. (2021). Tectonic evolution of the Sichuan Basin, Southwest China. *Earth-Science Rev.* 213, 103470. doi:10.1016/j.earscirev.2020.103470

Liu, T. J., Wang, X. L., Wang, Z. T., Santosh, M., Liu, X. F., Ju, P. C., et al. (2023). Depositional response to the emeishan mantle plume: evidence from the eastern Sichuan Basin, South China. *Int. Geol. Rev.* 65 (21), 3311–3328. doi:10.1080/00206814.2023.2185821

Lu, Y. Y., Zhang, H. D., Zhou, Z., Ge, Z. L., Chen, C. J., Hou, Y. D., et al. (2021). Current status and effective suggestions for efficient exploitation of coalbed methane in China: a review. *Energy and Fuels* 35 (11), 9102–9123. doi:10.1021/acs.energyfuels.1c00460

Luo, P. Y., and Zhu, S. Y. (2023). Theoretical and technical fundamentals of a 100 billion-cubic-meter-scale large industry of coalbed methane in China. *Acta Pet. Sin.* 44 (11), 1755–1763. (in Chinese, with English abstract).

Luo, J. X., He, Y. B., and Wang, R. (2014). Lithofacies palaeogeography of the late Permian wujiaping Age in the middle and upper Yangtze region, China. *J. Palaeogeogr.* 3 (4), 384–409.

Ming, Y., Sun, H. F., Tang, D. Z., Xu, L., Zhang, B. J., Chen, X., et al. (2024). Potential for the production of deep to ultradeep coalbed methane resources in the Upper Permian longtan formation, Sichuan Basin. *Coal Geol. and Explor.* 52 (2), 102–112. (in Chinese, with English abstract).

Qin, Y. (2018). Research progress of symbiotic accumulation of coal measure gas in China. *Nat. Gas. Ind.* 38 (4), 26–36. (in Chinese, with English abstract).

Qin, Y. (2021). Strategic thinking on research of coal measure gas accumulation system and development geology. *J. China Coal Soc.* 46 (8), 2387–2399. (in Chinese, with English abstract).

Qin, Y. (2023). Progress on geological research of deep coalbed methane in China. *Acta Pet. Sin.* 44 (11), 1791–1811. (in Chinese, with English abstract).

Qu, T., Huang, Z. L., Wang, R., Tan, S. Z., Li, Z. Y., Guo, X. B., et al. (2021). Development characteristics and controlling factors of coal-measure source rocks in the global tethys region. *Coal Geol. and Explor.* 49 (5), 114–131. (in Chinese, with English abstract).

Sang, S. X., Han, S. J., Liu, S. Q., Zhou, X. Z., Li, M. X., Hu, Q. J., et al. (2022). Comprehensive study on the enrichment mechanism of coalbed methane in high rank reservoirs. *J. China Coal Soc.* 47 (1), 388–403. (in Chinese, with English abstract).

Shao, L. Y., Wang, X. T., Lu, J., Wang, D. D., and Hou, H. H. (2017). A reappraisal on development and prospect of coal sedimentology in China. *Acta Sedimentol. Sin.*, 1016–1031. (in Chinese, with English abstract).

Tong, C. G. (2000). Relationship between neotectonic movement and structural evolution and gas pools formation of sichuan basin. *J. Chengdu Univ. Technol.* 27 (2), 123–130. (in Chinese, with English abstract).

Vinson, D. S., Blair, N. E., Ritter, N. E., Martini, A. M., and Mclntosh, J. C. (2019). Carbon mass balance,isotopic tracers of biogenic methane,and the role of acetate in coal beds:powder river basin (USA). *Chem. Geol.* 530, 119329–329. doi:10.1016/j.chemgeo.2019.119329

Wang, E. Z., Guo, T. L., Li, M. W., Xiong, L., Dong, X. X., Zhang, M. X., et al. (2022). Depositional environment variation and organic matter accumulation mechanism of marine-continental transitional shale in the Upper Permian longtan formation, sichuan basin, SW China. *ACS Earth Space Chem.* 6 (9), 2199–2214. doi:10.1021/acsearthspacechem.2c00101

Wang, Y., Zhang, H. Y., Zhu, Y. M., Chen, S. B., Cao, Q. S., Huang, M. L., et al. (2024). Sedimentary environment and major controlling factors of organic matter-rich shale from the wufeng-longmaxi formation in eastern Sichuan Basin,China. *Front. Earth Sci.* 18 (3), 649–670. doi:10.1007/s11707-024-1108-z

Wang, Q., Tian, C., Luo, C., Zhang, J. Y., Yang, X., Wu, W., et al. (2025). Characteristics and exploration prospects of coal-rock gas reservoirs in Permian longtan formation in suining-hejiang area, Sichuan Basin. *Lithol. Reserv.* 37 (4), 26–37. (in Chinese, with English abstract).

Wei, H. Y. (2012). Productivity and redox proxies of palaeo-oceans: an overview of elementary geochemistry. *Sediment. Geol. Tethyan Geol.* 32 (2), 76–88. (in Chinese, with English abstract).

Wen, L., Luo, B., Sun, H. F., Zhang, B. J., Ming, Y., Chen, X., et al. (2024a). Geological characteristics and resources potential of deep coal-rock gas reservoir in the Upper Permian longtan formation of the Sichuan Basin. *Nat. Gas. Ind.* 44 (10), 22–32. (in Chinese, with English abstract).

Wen, L., Ming, Y., Sun, H. F., Zhang, B. J., Chen, X., Chen, S. D., et al. (2024b). Geological characteristics and exploration potential of deep coalbed methane in the Permian longtan formation, Sichuan Basin: a case study of well NT1H. *Oil and Gas Geol.* 45 (6), 1678–1685. (in Chinese, with English abstract).

Xie, W. R., Wen, L., Wang, Z. C., Hao, Y., Xin, Y. G., Wu, S. J., et al. (2024). Types of unconventional marine resources and favorable exploration directions in the permian-Middle Triassic of the Sichuan Basin. *Nat. Gas. Geosci.* 35 (6), 961–971. (in Chinese, with English abstract).

Xu, F. Y., Hou, W., Xiong, X. Y., Xu, B. R., Wu, P., Wang, H. Y., et al. (2023a). The status and development strategy of coalbed methane industry in China. *Petroleum Explor. Dev.* 50 (4), 765–783. doi:10.1016/s1876-3804(23)60427-6

Xu, F. Y., Yan, X., Li, S. G., Xiong, X. Y., Wang, Y. X., Zhang, L., et al. (2023b). Theoretical and technological difficulties and countermeasures of deep CBM exploration and development in the eastern edge of ordos basin. *Coal Geol. and Explor.* 51 (1), 115–130. (in Chinese, with English abstract).

Xu, F. Y., Nie, Z. H., Sun, W., Xiong, X. Y., Xu, B. R., Zhang, L., et al. (2024). Theoretical and technological system for highly efficient development of deep coalbed methane in the eatern edge of erdos basin. *J. China Coal Soc.* 49 (1), 528–544. (in Chinese, with English abstract).

Yuan, H. F., Zhang, B. J., Kuang, M. Z., Zhang, X. H., Li, W. J., Peng, H. L., et al. (2025). Coupling of tectonic-sedimentary differentiation and emeishan mantle plume during the middle Permian maokouan in Sichuan Basin. *J. Palaeogeogr. Chin. Ed.* 27 (3), 560–577. (in Chinese, with English abstract).

Zhang, Y. C., Li, C. L., Hong, X. F., Yuan, Y. C., Wang, X. H., Huang, Y. A., et al. (1993). *Sedimentary environments and coal accumulation of late Permian coal formation in southern sichuan, China*, 1993. Guiyang: Guizhou Science and Technology Press, 204. (in Chinese, with English abstract).

Zhang, S. Q., Abdallah, K. B., Li, L., Hamdi, E., and Liu, J. (2025). Multiphase flow controlled by synergistic injection-production pressure: enabling CO_2 geo-sequestration with additional gas recovery from vertically heterogeneous depleted shale reservoirs. *Fuel* 398, 135591. doi:10.1016/j.fuel.2025.135591

Zou, C. N., Yang, Z., Huang, S. P., Ma, F., Sun, Q. P., Li, F. H., et al. (2019). Resource types, formation, distribution and prospects of coal-measure gas. *Petroleum Explor. Dev.* 46 (3), 451–462. doi:10.1016/s1876-3804(19)60026-1